THE JOURNAL OF COMPARATIVE NEUROLOGY 343:609–616 (1994)

Synaptic Organization of Regenerated Retina in the Goldfish

PETER F. HITCHCOCK AND PAUL CIRENZA
Departments of Ophthalmology and Anatomy and Cell Biology, The University of Michigan School of Medicine, Ann Arbor, Michigan 48105

ABSTRACT

In the adult goldfish, any manipulation that significantly depletes retinal neurons stimulates neurogenesis and the regeneration of nearly normal retina. We sought to determine the extent to which the regenerated neurons formed normal synaptic connections. We used qualitative and quantitative electron microscopy to compare the organization of the synaptic layers in regenerated and normal retinas. In eight eyes, a small patch of retina was surgically excised, stimulating regeneration of new retina in its place. Animals were killed 16–20 weeks after surgery. Qualitative comparisons of the synaptic architecture of photoreceptor terminals in the outer plexiform layer and quantitative comparisons of the synaptic organization in the inner plexiform layer were made between the patch of regenerated retina and an adjacent intact site. In the regenerated outer plexiform layer, cone pedicles and rod spherules were not arranged as regularly as normal, but they formed normal-appearing synaptic contacts. In the regenerated inner plexiform layer, with one exception, the quantitative descriptors of the synaptic organization in the normal and regenerate were not significantly different: The planimetric and numerical densities of the synapses, number of synapses/inner retinal neuron, and, with the exception of the bipolar terminals in the inner plexiform layer, and synapse depth profiles were similar. These data suggest that 1) relatively normal synaptic connections are recreated during regeneration, 2) the cellular mechanisms that guide synaptogenesis during development act during retinal regeneration, and 3) the physiological response properties of regenerated neurons should be comparable to that found in the normal retina.

Key words: synaptogenesis, regeneration, electron microscopy, outer plexiform layer, inner plexiform layer

The retina is a part of the central nervous system that resides outside the cranium but retains all the properties of the more proximal parts of the brain (Dowling, 1987). In the teleost fish, this tissue is unique in that it can regenerate new neurons following injury (for review, see Hitchcock and Raymond, 1992). Any manipulation that significantly depletes the population of extant, differentiated neurons stimulates their replacement by regenerative neurogenesis (Lombardo, 1968, 1972; Maier and Wolburg, 1979; Kurz-Isler and Wolburg, 1982; Raymond et al., 1988; Braisted and Raymond, 1992; Hitchcock et al., 1992; Hitchcock and VanDeRyt, 1994). Convincing, albeit circumstantial, evidence (Raymond et al., 1988) indicates that regenerated retinal neurons derive from an intrinsic population of primitive neuroepithelial cells. These cells, known as rod precursors, normally give rise to rod photoreceptors only (Johns and Fernald, 1981; Raymond, 1985). Injury to the retina, however, stimulates the rod precursors or their progeny to proliferate, alter their rod-only fate, and produce neurons of all types.

Recently, we have begun studying retinal regeneration in the goldfish following a surgical lesion (Hitchcock et al., 1992; Hitchcock and VanDeRyt, 1994). Within a few days of removing a small piece of retina, a cluster of proliferating cells, which we called a blastema (Hitchcock et al., 1992), forms at the margin of the retinal wound and migrates centripetally into the lesion, appositionally adding new retina to the old. The missing retina is replaced in about 4–6 weeks. This experimental approach allows one to make within-eye comparisons between intact retina and retina that has regenerated. In the present study, electron microscopy was used to compare the synaptic organization of normal and regenerated retina; the outer plexiform layer (OPL) was studied qualitatively, whereas several numeric descriptors were used to study the inner plexiform layer

Accepted December 8, 1993.

Address reprint requests to Peter F. Hitchcock, Kellogg Eye Center, 1000 Wall Street Ann Arbor, MI 48105.

(IPL) quantitatively. These data have been presented in preliminary form elsewhere (Hitchcock and Cirenza, 1993).

MATERIALS AND METHODS

Prior to all surgeries and sacrifice, animals were anesthetized in tricaine methanesulfonate (MS 222). Animals were killed by exsanguination. Retinal lesions were made in eight eyes from six juvenile goldfish, *Carassius auratus* (7.2 cm, mean standard body length; 2.6 mm, mean lens diameter). Procedures similar to those described previously were used (see Hitchcock et al., 1992). Briefly, the eye was rotated ventrally, the conjunctiva was dissected away from the dorsal aspect of the globe, and three full-thickness cuts were made through the dorsonasal quadrant to create a tongue-shaped flap. The flap was reflected outward, and the retina, generally 1–2 mm^2, was gently separated from the underlying pigmented epithelium, cut at its base, and removed. A single stitch of ophthalmic suture was used to close the sclera.

Eyes were enucleated from light-adapted animals 16–20 weeks postlesion. For each, the lens and cornea were removed and the eye cup was fixed by immersion for 1 hour in 2.5% glutaraldehyde/2.0% paraformaldehyde in Sörensen's buffer, pH 7.2. After the eye was rinsed in buffer, the patch of regenerated retina was identified by the mottled appearance of the underlying pigmented epithelium and the fascicles of ganglion cell axons along its boundary (Hitchcock et al., 1992). The regenerate and an adjacent piece of the normal retina were excised and cut into small blocks to be processed for electron microscopy (see Hitchcock, 1989, 1993). Blocks were postfixed for 1 hour in 0.5% osmium tetroxide, stained en bloc overnight in uranyl acetate, dehydrated in ethanol and propylene oxide, and infiltrated and embedded in POLYBED 812.

Thick sections (0.5 μm), cut perpendicular to the retinal layers from each of the 16 blocks, were stained with toluidine blue, viewed with a light microscope, and in each the area to be sampled by electron microscopy was identified. For sections of normal retina, all areas of the section were considered equivalent. For the regenerated retinas, only cell-free stretches of the IPL were selected. Those sites where the inner nuclear and ganglion cell layers had fused (see Hitchcock, et al., 1992) were excluded.

The planimetric density of inner retinal neurons was estimated by counting nuclei in the inner nuclear (excluding horizontal cells) and ganglion cell layers along a 270 μm length of retina that included the regions selected for electron microscopy. (There was no difference in the average size of the nuclei in the normal and regenerated retinas; therefore, these counts were not corrected for split nuclei.) The neuronal planimetric density was determined by dividing their number by the area sampled (270 × 0.5 μm). The number of synapses/nucleus was calculated by dividing the synaptic planimetric density (see below) by the nuclear planimetric density.

Thin sections (silver-gold interference colors) were cut and collected on formvar-coated, one-hole copper grids and stained with lead citrate. Sections were viewed and photographed with a Philips CM-10 electron microscope. From one thin section from each of the 16 blocks, 30 overlapping photomicrographs of the IPL were taken (by P.C.) and printed at a final magnification of ×13,230. The photomicrographs were randomly ordered and scored for synapses (by P.F.H.) and then grouped according to animal and treatment and assembled into mosaics. The planimetric density of synapses, defined as the number of synapses per unit area that project onto a plane parallel to the inner limiting membrane, was calculated by dividing the number of synapses counted by the product of IPL length × section thickness (0.09 μm). The numerical density, defined as the number of synapses per unit volume, was calculated by dividing the number of synapses counted by the product of IPL length × section thickness (0.09 μm) × IPL height. Synapse depth profiles were generated by dividing the IPL in each mosaic into ten equally spaced, horizontal laminae and determining the percentage of each synapse type present in each lamina. Statistical comparisons were made either by the Wilcoxon matched-pairs signed ranks test or by a χ^2 comparison.

RESULTS

Figure 1 shows light photomicrographs of sections from normal (Fig. 1A) and regenerated (Fig. 1B) retinas. Subtle but consistent differences distinguish the two. Occasional fusions occur between the cellular laminae in the regenerated retinas, and these retinas tend to be thinner than normal. This latter feature is because regenerated retinas have fewer rod photoreceptor nuclei in the outer nuclear layer and a thinner plexus of horizontal cell axons in the inner nuclear layer. The continual addition of new rods and the enlargement of the horizontal cell axons are long-term, growth-related changes that occur in the normal retina (Johns, 1982; Raymond, 1990) but are not found in the regenerated retina after only 20 weeks postlesion (Hitchcock et al., 1992).

Outer plexiform layer

Our qualitative assessment of the OPL was based on light microscopic inspection of thick sections from each of the retinas studied and electron microscopic inspection of thin sections from a subset of these retinas. In the normal retina, the OPL consists of large, pyramidal cone pedicles and smaller, round or oval rod spherules that fill the intervening spaces. These terminals lie in a narrow plane, opposite the elongated somata of the horizontal cells, which lie in the inner nuclear layer. Ultrastructurally, each contains ribbon organelles and small, clear synaptic vesicles that form a halo around the ribbons and are also scattered throughout the terminal. As is illustrated in Figure 2, the two types of terminals are easily distinguished. Cone pedicles (Fig. 2A,B) are electron lucent and contain numerous ribbon organelles, and each is invaginated by numerous postsynaptic processes of bipolar and horizontal cells. Rod spherules (Fig. 2C,D), in contrast, are electron dense; contain single, long ribbon organelle; and are contacted by relatively few postsynaptic processes (see Stell, 1967, for more complete descriptions).

In the regenerate, the OPL is somewhat disorganized. The cone pedicles appear smaller, less regularly spaced, and occasionally misoriented. The rod spherules, although fewer in number, occupy the space between the cone pedicles as in the normal retina. The synaptic connections formed by individual terminals, however, appear normal. Regenerated cone pedicles (Fig. 2B) contain ribbon organelles and contact numerous postsynaptic processes, some of which invaginate the walls of the terminal, characteristic of horizontal cell spinules (see Wagner and Djamgoz, 1993). Regenerated rod spherules (Fig. 2D) contain a single ribbon organelle

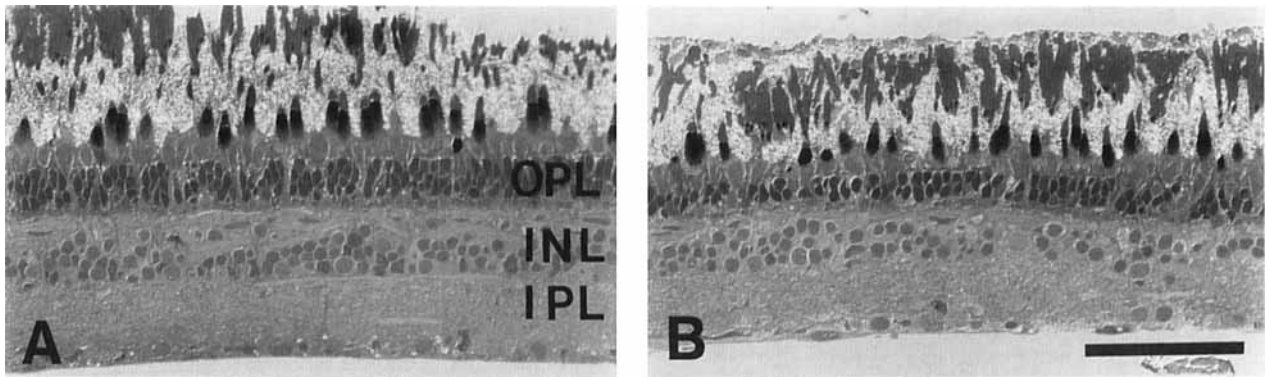

Fig. 1. Light photomicrographs of normal (**A**) and regenerated (**B**) retina. ONL, outer nuclear layer; INL, inner nuclear layer; IPL, inner plexiform layer. Scale bar = 50 μm.

surrounded by presumptive bipolar and horizontal cell processes cut in cross section.

Inner plexiform layer

The quantitative data were collected from photomosaics of the IPL that covered an average of 2,858 and 2,641 μm^2 in the normal and regenerated retinas, respectively. Each contained between 85–166 conventional and 9–45 ribbon synapses. Measurements of synapse lengths (see Dubin, 1970) from the first four pairs of mosaics revealed that there was no difference between size of the synapses in normal and regenerated retinas. Therefore, we made no stereological corrections of our synapse counts. Synapses and/or terminals were identified according to the general criteria outlined by Witkovsky and Dowling (1969), Dubin (1970), and Holmgren-Taylor (1983) and were divided into four categories based on their morphology and postsynaptic partners: 1) amacrine cell synapses that contact amacrine cell processes or ganglion cell dendrites, 2) amacrine cell synapses that contact bipolar cell terminals, 3) bipolar cell synapses, and 4) terminals (from amacrine cells) that contain large, dense-cored vesicles. Figure 3 shows examples of synapses within in the IPL. Amacrine cell synapses (Fig. 3A) were identified by the absence of any presynaptic organelles, the relatively small size of the terminal, and the clustering of small, agranular vesicles adjacent to a relatively electron-dense presynaptic membrane. This group actually consists of synapses from three different sources: amacrine cells, interplexiform cells, and retinal efferents. However, since the amacrine cell synapses are numerically predominant, we made no attempt to distinguish the other types. Bipolar cell synapses (Fig. 3B) were identified by the presence of a pentalaminar ribbon organelle surrounded by a halo of agranular vesicles adjacent to an electron-dense presynaptic membrane that was generally apposed to two postsynaptic processes. Dense-cored vesicles (Fig. 3C) were identified by their relatively large size, spherical shape, and a distinct dense center surrounded by a pale halo. Only terminals that contained both small, agranular vesicles and two or more dense-cored vesicles were scored. Dense-cored vesicles are found in amacrine cells and are characteristic of cells that contain neuroactive peptides such as substance P or somatostatin (e.g., Marshak et al., 1984; Yazulla et al., 1984, 1985; see also Pickel, 1985).

Table 1 shows the averaged data from the IPLs of normal and regenerated retinas. The planimetric density of regenerated amacrine synapses was slightly lower than control values (10.18 vs. 11.59 synapses/μm^2); however, this difference was not statistically significant. Of the eight regenerated retinas, five had synaptic densities below the normal values, whereas three had densities above. The planimetric densities of the bipolar synapses were also not significantly different, but here the density was slightly higher in the regenerated retina than in the normal one (2.12 vs. 1.83 synapses/μm^2). The numerical density of the amacrine cell synapses was virtually identical in the regenerated and normal retinas (0.47 vs. 0.46 synapses/μm^3), whereas the density of the ribbon synapses was again slightly higher but was not significantly different in the regenerate (0.11 vs. 0.09 synapses/μm^3). Similar to the planimetric and numerical synapse densities, there was no significant difference in the number of synapses/nucleus in the normal and regenerated retinas.

Figure 4 illustrates the depth profile of synapses in normal (dashed lines) and regenerated (solid lines) retinas. Statistical comparisons were made by collapsing the values of each profile into three bins (illustrated in Fig. 5), the inner and outer 30% (0–30% depth and 70–100% depth, respectively) and the middle 40% (30–70% depth), and performing a 2×3 χ^2 comparison. Figure 4A illustrates the depth profile of amacrine cell synapses that contact all nonbipolar processes. In the normal retina, they have a relatively flat profile that falls off gradually at the inner and outer 20%. The depth profile of the regenerated synapses closely approximates the normal profile, and there was no statistical difference between the two. Figure 4B illustrates the depth profile of amacrine cell synapses that contacted bipolar cell terminals. These are a small minority (about 15%) of the total population of amacrine cell synapses in the IPL. Their depth profile is bimodal and, not surprisingly, roughly approximates the profile of both the normal and regenerated bipolar cell synapses (cf. Fig. 4B,C). The profile of the regenerated synapses, although bimodal, did not match the normal profile at the 30% and 60–70% depths and as a result was significantly different from normal. Figure 4C illustrates the depth profile for bipolar cell synapses. These synapses have a bimodal distribution within the IPL, with peaks at the 30% and 80% depths (see also Yazulla, 1981; Yazulla and Studholme, 1987). This

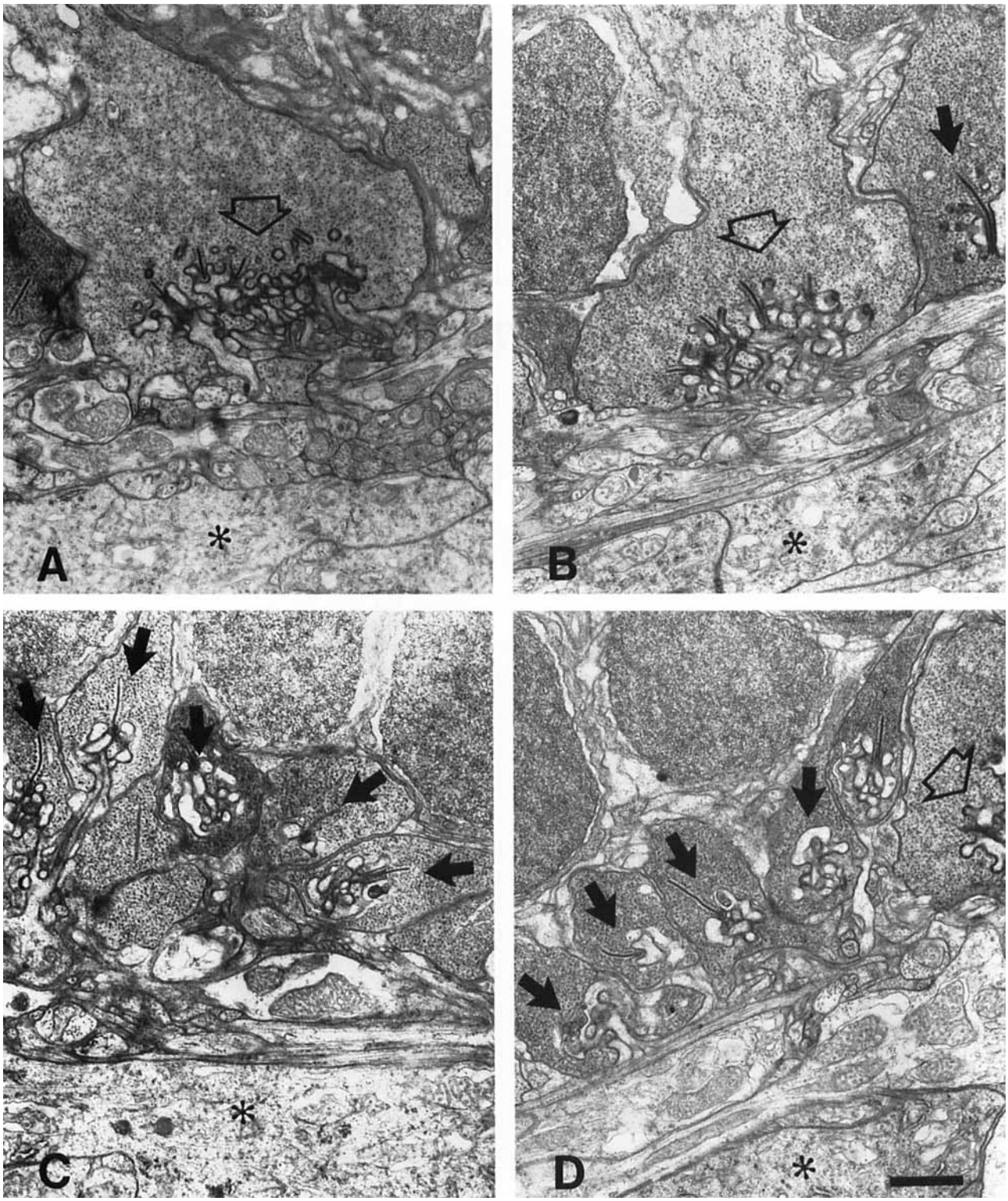

Fig. 2. Electron photomicrographs of synapses within the OPL. **A,B:** Cone pedicles in normal and regenerated retina, respectively. **C,D:** Rod spherules in normal and regenerated retina, respectively. Large, open arrows identify synaptic contacts made by the cone pedicles. Small, solid arrows identify synaptic contacts made by the rod spherules. Asterisks mark somata of horizontal cells. Scale bar = 1.0 μm.

probably corresponds to the centers of the ON and OFF sublaminae within the IPL (Famiglietti and Kolb, 1976; Famiglietti et al., 1977). The depth profile of the regenerated synapses had a nearly bimodal distribution as well, but the peak in the inner one-half of the IPL was at the 60–70% depth, in contrast to the normal value of about 80%, and

this was sufficient to make these depth profiles significantly different. The shift in the depth profile of the regenerated bipolar synapses is not likely due to our inability to accurately identify the boundaries of the IPL in the regenerate, since all the depth profiles from the normal and regenerated retinas matched closely at the inner and outer boundaries. Figure 4D illustrates the depth profiles for the amacrine cell terminals that contain dense-cored vesicles. Marshak et al. (1988) showed that these terminals are encountered most frequently near the boundaries of the IPL, particularly the innermost one, and they are relatively rare in the center. This observation was confirmed here. The depth profile of the regenerated terminals almost perfectly matched the normal one, and there was no statistical difference between the two.

TABLE 1.

Synapse type	Normal (n = 8)	Regenerated (n = 8)
Planimetric density (No./μm^2)		
Conventional	11.59	10.18[1]
Ribbon	1.83	2.12[1]
Numerical density (No./μm^3)		
Conventional	0.46	0.47[1]
Ribbon	0.09	0.11[1]
Synapses/Nucleus		
Conventional	18.81	16.81[1]
Ribbon	2.80	3.48[1]

[1] $P > 0.05$ (Wilcoxon matched-pairs signed ranks test).

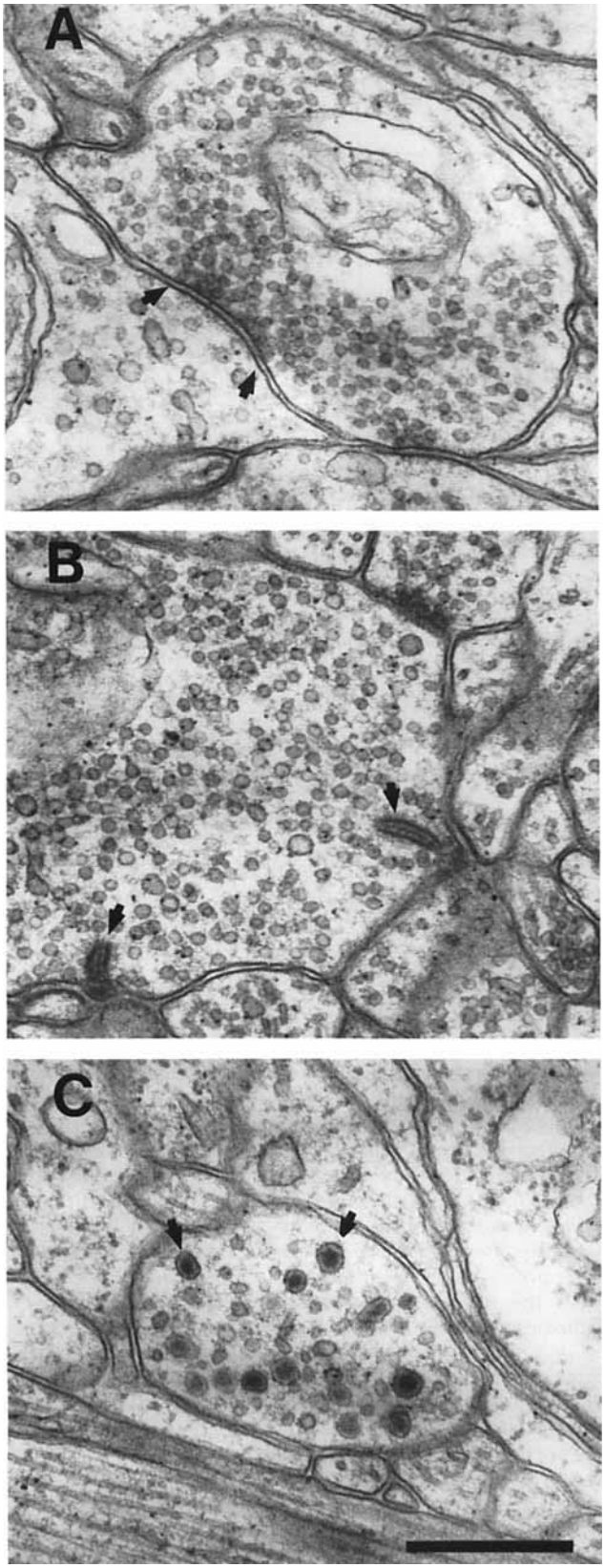

DISCUSSION

There is a wealth of descriptive anatomical data on the synaptic organization of the fish retina. Numerous studies have detailed the morphology of terminals in both plexiform layers, the circuitry they participate in, and their neurochemical identity (e.g., Stell, 1967; Witkovsky and Dowling, 1969; Holmgren-Taylor, 1983; Marshak et al., 1984; Yazulla et al., 1984, 1985, 1987). These data served as a template against which we could compare our data from normal retina, and they allowed us to perform a relatively fine-grained analysis of the regenerated retina using only standard electron microscopy. Our observations of normal retina agree well with these earlier studies, regarding both the various types of synapses present (Stell, 1967; Witkovsky and Dowling, 1969; Holmgren-Taylor, 1983) and their distributions throughout the depth of the IPL (Yazulla, 1981; Yazulla and Studholme, 1987; Marshak et al., 1988).

Our comparisons between the normal and regenerated retinas indicate that, in the regenerate, the synaptic organization of both plexiform layers is virtually normal. In the OPL, the cone terminals were relatively large and electron lucent and were contacted by numerous invaginating processes. Rod terminals were smaller and electron dense and were contacted by relatively few processes that appeared to envelope the ribbon organelle (see Stell, 1967). Similarly, in the IPL, most of the quantitative data from the regenerates were not significantly different from normal. In those regions of the regenerated IPL not interrupted by laminar fusions, the planimetric density, the numerical density, and

Fig. 3. Electron photomicrographs of synapses within the IPL. **A:** Synapses from an amacrine cell onto a nonbipolar cell process. The arrowheads indicate the extent of the synaptic contact. A second synapse made by this terminal can be seen at lower right. **B:** Two synapses from a bipolar cell axon. The arrowheads indicate synaptic ribbons. **C:** A synaptic terminal (from an amacrine cell) that contains dense-cored vesicles, two of which are indicated with arrowheads. Scale bar = 0.5 μm.

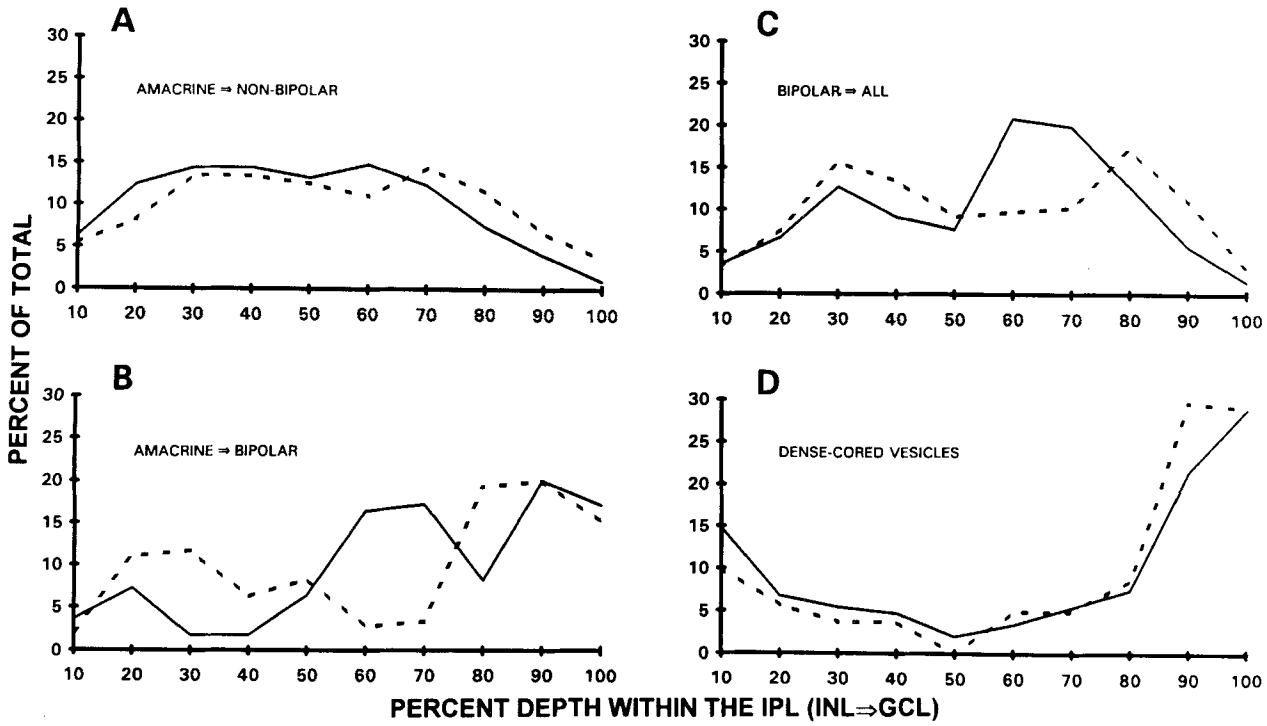

Fig. 4. Depth profiles of synapses within the IPL from normal (dashed lines) and regenerated (solid lines) retinas. Plotted on the ordinate is the proportion of that population of synapses found in each laminae. **A:** Amacrine cell synapses that contact nonbipolar cell processes (n = 1,026 and 840, normal and regenerated, respectively). **B:** Amacrine cell synapses that contact bipolar cell terminals (n = 145 and 110, normal and regenerated, respectively). **C:** Bipolar cell synapses (n = 186 and 197, normal and regenerated, respectively). **D:** Terminals that contain dense-cored vesicles (n = 162 and 177, normal and regenerated, respectively).

the number of synapses/inner retinal neuron were not significantly different from normal. However, because the laminar fusions represent small islands of the inner nuclear layer that erupt into the ganglion cell layer, the total number of synapses in the entire piece of regenerated retina is likely to be less than that for an equivalent area of normal retina.

The only statistically significant difference we observed between the normal and the regenerated IPL was the slight sclerad displacement in the regenerate of bipolar terminals in the inner IPL and those amacrine cell synapses that contact them. We have no explanation for this result, but we think it significant that the two profiles change in tandem. This suggests that amacrine cells that normally contact bipolar terminals in the inner IPL did so in the regenerate, despite their relative mislocation. With this exception, the synapse depth profiles illustrated in Figure 4 suggest that the processes of amacrine cells in the regenerate should have normal, cell type-specific stratification patterns. Although we have not systematically surveyed this, the normal stratification pattern of the dopaminergic cells (Hitchcock and VanDeRyt, 1994) and the normal depth profile of the terminals containing dense-cored vesicles, which are found in only a few cell types (see Marshak et al., 1984; Yazulla et al., 1985), suggest that the neurochemical stratification (see Marc, 1986) in the regenerate is normal.

Two recent studies quantitatively compared the neuronal organization of the normal and regenerated retina. In the first (Hitchcock et al., 1992), the planimetric density of regenerated neurons, estimated from counts made in sections, showed that the density of regenerated, nonrod neurons approximated that of the normal retina. Lesions made in retinas that varied systematically in size and cell density [in fish, the density of nonrod neurons decreases with increasing retinal area (see Johns, 1982; Kock, 1982)] resulted in a systematic, parallel decrease in the planimetric density of the regenerated neurons. In the second study (Hitchcock and VanDeRyt 1994), the planimetric density of regenerated dopaminergic interplexiform cells was directly measured in whole-mounted retinas. The regenerated neurons and their processes formed relatively disordered "mosaics," although the stratification pattern of their dendrites within the IPL appeared normal. These studies led to three conclusions. First, during regeneration, the cellular mechanisms that control the expression of neuronal phenotype as a function of radial location, i.e., inner vs. outer retina, are normal; second, the planimetric density of regenerated neurons matches that of the surrounding normal one; and, third, the dendritic stratification pattern of regenerated neurons is normal, but the mechanisms that establish the tangential arrangement of the somata and their processes are either absent or compromised.

To the conclusions given above we can now add the following from the present study. First, the normal synaptic organization in the retina is recreated during regeneration; therefore, similar cellular and molecular mechanisms likely guide both de novo and regenerative synaptogenesis. Once the fate of a regenerated cell is determined, it engages the normal phenotype-specific pattern of process outgrowth and transports synaptic proteins and organelles or their synthetic components (Oswald, 1987), to pre- and postsynaptic sites, and there assembles normal synaptic junctions, both in kind and number. Second, what distinguishes

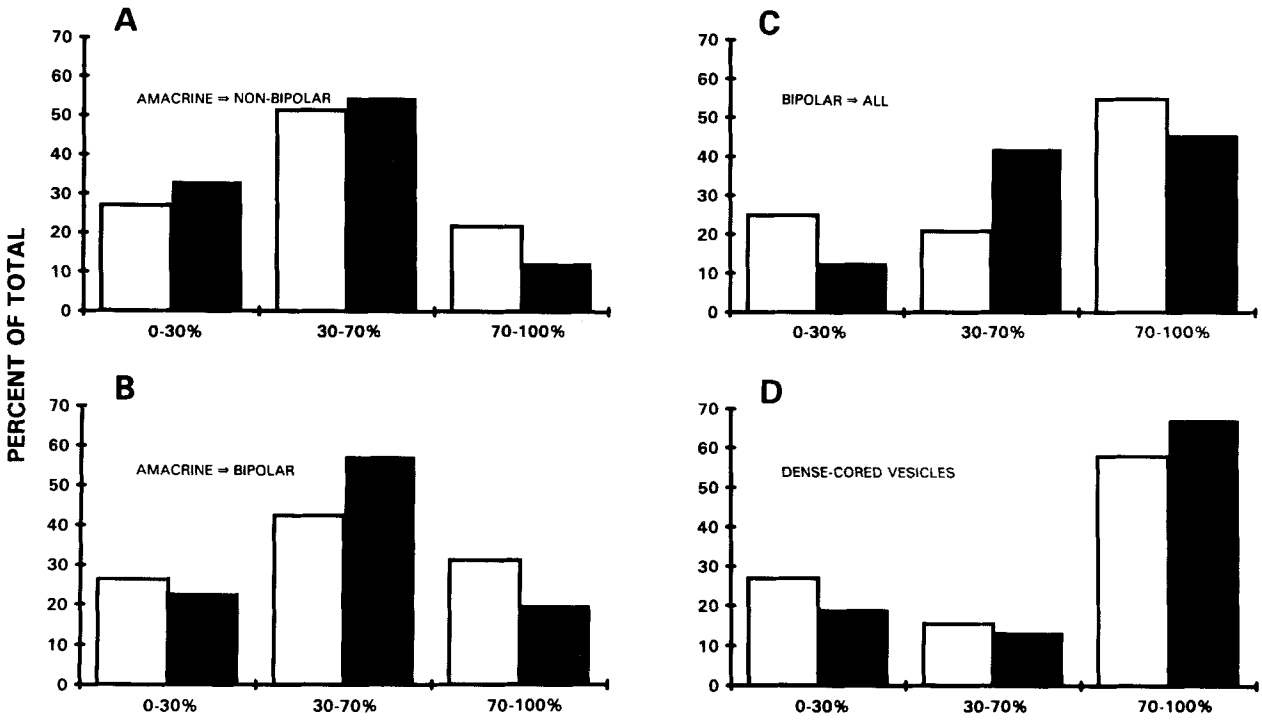

Fig. 5. Depth profiles of synapses within the IPL from normal (open bars) and regenerated (solid bars) retinas replotted as histograms. The data for each were collapsed into three bins for the purpose of statistical analysis (see Results). **A:** Amacrine cell synapses that contact nonbipolar cell processes. **B:** Amacrine cell synapses that contact bipolar cell terminals. **C:** Bipolar cell synapses. **D:** Terminals that contain dense-cored vesicles.

retinal development from regeneration is that the latter occurs on a much foreshortened time scale. The number of synapses at any retinal site results from a slow accretion of new ones over time (Fisher and Easter, 1977). During regeneration, the number of synapses goes from zero to a value equal to the surrounding, much older piece of retina within the space of only a few weeks. Although not tested here, this suggests that similar to regenerative neurogenesis (Hitchcock et al., 1992), regenerative synaptogenesis matches the number and density of synapses to that in the surrounding, normal retina.

What might control the number of synapses formed during regeneration? Studies of the mature CNS suggest that synapse number in a neuropil may be regulated by the size of the available postsynaptic surfaces (Purves and Hume, 1981; Nicol and Meinertzhagen, 1982; Sargent, 1983; see also Hitchcock, 1993). Our earlier data (Hitchcock et al., 1992) suggest that neurons are regenerated on a scale matched to the surrounding retina. If the size of regenerated neurons matches that of those in the surrounding, normal retina, the number of synapses in the regenerate might simply reflect the amount of available postsynaptic space. Although not tested here, this suggests that the synaptic planimetric density in the regenerate, as in the normal retina (Fisher and Easter, 1979), should be greater in large, old fish than in small, young ones.

To the extent that the structural features of the OPL and quantitative features of the IPL in the regenerate are indicative of normal retinal circuitry, our data suggest that the receptive field properties of regenerated retinal neurons should be normal. Consistent with this, electroretinogram recordings (Sarthy and Lam, 1983; Mensinger and Powers, 1993) have shown that regenerated retinas generate normal, albeit smaller in amplitude, photoreceptor (A-wave) and bipolar (B-wave) potentials in response to whole-field flashes of light. Although this technique does not measure the response of single cells, normal waveforms are indicative of normal cellular response properties. Investigating the light responses of individual regenerated retinal neurons will provide insights into the functional state of regenerated retina and may provide further insights into the mechanisms that control synaptogenesis in regenerating retina.

ACKNOWLEDGMENTS

The authors thank D. Marshak, M.K. Powers, P.A. Raymond, and D.A. Thompson, S. Boucher, and A. Morisette for reading and commenting on earlier versions of this paper. Technical support was provided by M. Gillett and secretarial support was provided by D. Giebel. S.S. Easter, Jr. translated the Lombardo papers. This study was supported by NIH (NEI) grants EY07060 and EY07003 (CORE).

LITERATURE CITED

Braisted, J.E., and P.A. Raymond (1992) Regeneration of dopaminergic neurons in goldfish retina. Development *114*:913–919.

Dowling, J.E. (1987) The Retina. Cambridge, MA: The Belknap Press of Harvard University Press.

Dubin, M.S. (1970) The inner plexiform layer of the vertebrate retina: A quantitative and comparative electron microscopic analysis. J. Comp. Neurol. *140*:479–506.

Famiglietti, E.V. Jr., and H. Kolb (1976) Structural basis for ON-and OFF-center responses in retinal ganglion cells. Science *194:*193–195.

Famiglietti, E.V. Jr., A. Kaneko, and M. Tachibana (1977) Neuronal architecture of on and off pathways to ganglion cells in carp retina. Science *198:*1267–1269.

Fisher, L.J., and S.S. Easter Jr. (1979) Retinal synaptic arrays: Continuing development in the adult goldfish. J. Comp. Neurol. *185:*373–380.

Hitchcock, P.F. (1989) Morphology and distribution of synapses onto a type of large field ganglion cell in the retina of the goldfish. J. Comp. Neurol. *283:*177–188.

Hitchcock, P.F. (1993) Mature, growing ganglion cells acquire new synapses in the retina of the goldfish. Vis. Neurosci. *10:*219–224.

Hitchcock, P.F., and P.A. Raymond (1992) Retinal Regeneration. Trends Neurosci. *15:*103–108.

Hitchcock, P.F., and P. Cirenza (1993) Synaptic organization of the inner plexiform layer (IPL) in the regenerated retina of the goldfish. Neurosci. Abstr. *19:*55.

Hitchcock, P.F., and J.T. VanDeRyt (1994) Regeneration of the dopamine-cell mosaic in the retina of the goldfish. Vis. Neurosci. *11:* 209–217.

Hitchcock, P.F., K.J. Lindsey Myhr, S.S. Easter Jr., R. Mangione-Smith, and D. Dwyer Jones (1992) Local regeneration in the retina of the goldfish. J. Neurobiol. *23:*187–203.

Holmgren-Taylor, I. (1983) Synapses of the inner plexiform layer in the retina of cyprinid fish. Cell. Tissue Res. *229:*337–350.

Johns, P.R. (1982) Formation of photoreceptors in larval and adult goldfish. J. Neurosci. *2:*178–198.

Johns, P.R., and R.D. Fernald (1981) Genesis of rods in teleost fish retina. Nature *293:*141–142.

Kock, J.-H. (1982) Neuronal addition and retinal expansion during growth of the crucian carp eye. J. Comp. Neurol. *209:*264–274.

Kurz-Isler, G., and H. Wolburg (1982) Morphological study on the regeneration of the retina in the rainbow trout after ouabain-induced damage: Evidence of dedifferentiation of photoreceptors. Cell Tissue Res. *225:*165–178.

Lombardo, F. (1968) La rigenerazione della retina negli adulti di un teleosteo. Accad. Lincei-Rendiconti Sci. Fis. Mat. Nat. *45:*631–635.

Lombardo, F. (1972) Andamento e localizzazione delle mitosi durante le rigenerazione della retina di un teleosteo adulto. Accad. Lincei.-Rendiconti Sci. Fis. Mat. Nat. *53:*323–327.

Maier, W., and H. Wolburg (1979) Regeneration of the goldfish retina after exposure to different doses of ouabain. Cell Tissue Res. *202:*99–118.

Marc, R.E. (1986) Neurochemical stratification in the inner plexiform layer of the vertebrate retina. Vis. Res. *26:*223–238.

Marshak, D.W., T. Yamada, and W.K. Stell (1984) Synaptic contacts of somatostatin-immunoreactive amacrine cells in goldfish retina. J. Comp. Neurol. *225:*44–52.

Marshak, D., M. Ariel, and E. Brown (1988) Distribution of synaptic inputs onto goldfish retinal ganglion cell dendrites. Exp. Eye Res. *46:*965–978.

Mensinger, A.F., and M.K. Powers (1993) Visual function following surgical removal of retinal tissue. Invest. Ophthalmol. Vis. Sci. (Suppl.) *34:*1177.

Nicol, D., and I.A. Meinertzhagen (1982) Regulation in the number of fly photoreceptor synapses: The effects of alterations in the number of presynaptic cells. J. Comp. Neurol. *207:*45–60.

Pickel, V. (1985) General morphological features of peptidergic neurons. In. A. Björklund and T. Hokfelt (eds): Handbook of Chemical Neuroanatomy. New York: Elsevier, pp. 72–92.

Purves, D., and R.I. Hume (1981) The relation of postsynaptic geometry to the number of presynaptic axons that innervate ganglion cells. J. Neurosci. *1:*441–452.

Raymond, P.A. (1985) The unique origin of rod photoreceptors in the teleost retina. Trends Neurosci. *8:*12–17.

Raymond, P.A. (1990) Horizontal axon terminals in growing goldfish. Exp. Eye Res. *51:*675–684.

Raymond, P.A., M.J. Reifler, and P.K. Rivlin (1988) Regeneration of goldfish retina: Rod precursors are a likely source of regenerated cells. J. Neurobiol. *19:*431–463.

Sarthy, P.V., and D.M.-K. Lam (1983) Retinal regeneration in the adult newt, *Notophthalmus viridescens*: Appearance of neurotransmitter synthesis and the electroretinogram. Dev. Brain Res. *6:*99–105.

Sargent, P.B. (1983) The number of synaptic boutons terminating on *Xenopus* cardiac ganglion cells is directly correlated with cell size. J. Physiol. *343:*85–104.

Stell, W.K. (1967) The structure and relationships of horizontal cells and photoreceptor-bipolar synaptic complexes in goldfish retina. Am. J. Anat. *121:*401–432.

Wagner, J.-H., and M.B.A. Djamgoz (1993) Spinules: A case for retinal synaptic plasticity. Trends Neurosci. *16:*201–206.

Witkovsky, P., and J.E. Dowling (1969) Synaptic relationships in the plexiform layers of carp retina. Z. Zellforsch. *100:*60–82.

Yazulla, S. (1981) GABAergic synapses in the goldfish retina: An autoradiographic study of ^{3}H-muscimol and ^{3}H-GABA binding. J. Comp. Neurol. *200:*83–93.

Yazulla, S., and K.M. Studholme (1987) Ultracytochemical distribution of ouabain-sensitive, K^{+}-dependent, p-nitrophenylphosphatase in the synaptic layers of goldfish retina. J. Comp. Neurol. *261:*74–84.

Yazulla, S., J. Mosinger, and C. Zucker (1984) Two types of pyriform Ab amacrine cells in the goldfish retina: An EM analysis of [^{3}H]GABA uptake and somatostatin-like immunoreactivity. Brain Res. *321:*352–356.

Yazulla, S., K.M. Studholme, and C.L. Zucker (1985) Synaptic organization of substance P-like immunoreactive amacrine cells in goldfish retina. J. Comp. Neurol. *231:*232–238.

Yazulla, S., K.M. Studholme, and J.-Y. Wu (1987) GABAergic input to the synaptic terminals of mb_1 bipolar cells in the goldfish retina. Brain Res. *411:*400–405.